

Irradiation of pre-existing voids in nanocrystalline iron

M. Samaras^{a,*}, W. Hoeffelner^a, M. Victoria^{b,c}

^a NES, High Temperature Materials Group, Paul Scherrer Institute, CH-5232 Villigen PSI, Switzerland

^b Lawrence Livermore National Laboratory, P. O. Box 808, Livermore, CA 94551, USA

^c Polytechnic University of Madrid, José Gutierrez Abascal 2, 28006 Madrid, Spain

Abstract

Understanding the role of voids is an important issue in lifetime predictions of materials which are exposed to irradiation. In this paper, we investigate the effect of a pre-existing void structure embedded in a grain boundary in computer generated nanocrystalline Fe samples in terms of nearby primary cascade evolution using molecular dynamics simulations. Results indicate that the void and grain boundaries act as sinks to self interstitial atoms formed from nearby displacement cascades.

© 2006 Published by Elsevier B.V.

PACS: 31.15.Qg; 61.80.Az; 61.72.Bb

1. Introduction

The presence of voids and their activity is an important lifetime issue for materials subject to extreme conditions because of the swelling that can occur as a result of their formation. Voids nucleate through the agglomeration of large vacancy clusters which can form during the irradiation of a material. The existence of a large number of voids can cause a segregation process whereby self interstitial atoms (SIAs) are absorbed by dislocations and vacancies by voids [1]. As these voids absorb vacancies they grow larger and the materials will swell, rendering them useless for extreme condition applications.

Void swelling is one of the dominant effects of radiation at temperatures in the range $0.3\text{--}0.6 T_M$ (where T_M is the melting temperature) and therefore is an important issue to address for materials to be used in future advanced nuclear and fusion reactors. Experimentally, in bcc metals, voids are seen above stage III $0.15 T_M$ [2], whereas at low temperatures, no voids are observed in experiment [3] nor in single crystal simulations [4]. The lack of observed voids has been postulated to be due, not to their absence, but to the limited spatial resolution of the TEM. This postulation has led to the use of positron annihilation spectroscopy (PAS) measurements which were able to distinguish voids and ‘micro voids’ in body cubic centred (bcc) Fe [3].

The presence of sinks such as grain boundaries (GBs) influences the void swelling that can occur in a material [5]. Areas adjacent to GBs have been experimentally observed to contain denuded zones

* Corresponding author. Tel.: +41 56 310 4184; fax: +41 56 310 4595.

E-mail address: maria.samaras@psi.ch (M. Samaras).

[6,7] and areas adjacent to these denuded zones were found to have enhanced void swelling [6,8,9]. Theoretical models have been developed to describe the swelling behaviour of voids in terms of the production bias model (PBM) [10] where the 1D motion of SIA clusters to sinks is deemed an essential factor [11]. PBM has been used to explain the effect of grain size on void swelling [5] and the accumulations of voids near GBs [12]. Recently, the description of small SIA clusters [13,14] and larger SIA clusters, as a consequence of their interaction with nearby GBs [15,16] moving 1D/3D, using Molecular Dynamics (MD), has produced better agreement with void swelling effects seen near GBs in experiment than previous theoretical models [17]. Formation of large vacancy clusters during MD simulated irradiation in nanocrystalline (nc) bcc Fe has been seen in the vicinity of GBs due to the exodus of SIAs to the surrounding GB structure [18]. Simulations of displacement cascades near dislocations have been performed at high temperature and high dose irradiation with void swelling found due to a dislocation bias which acts as a sink to SIAs and produces an excess of vacancies necessary to produce voids [1].

To understand the involvement of SIAs in the microscopic stability of voids, it is necessary to understand SIA defect cluster formation and movement during irradiation in the presence of voids. This work presents preliminary results of displacement cascade simulations which are introduced in nc bcc Fe in the vicinity of a pre-existing void in the GB.

2. Method

The Voronoi method [20] is used to simulate a sample which contains a fully three dimensional grain boundary structure. The sample is constructed of 15 grains with 12 nm average sized grain diameters and contains 1.4 million atoms. The nc bcc Fe GB structure of a similar sample (constructed without a void) has been discussed and compared with fcc nanocrystal materials [18], whose structures have been extensively investigated [21,22]. To reach an equilibrium state, the sample is relaxed with molecular statics and then MD at 300 K for 150 ps. This sample contains an artificially created 2.9 nm (diameter) void situated at a GB triple junction (TJ). MD simulations at room temperature are performed. The simulation of a displacement cascade is introduced into the sample by choosing an atom called the primary knock-on atom (PKA) and placing an energy of 5, 10 or 20 keV with a direction on this PKA and watching

the evolution with time. The sample has periodic boundary conditions and heat is extracted using velocity rescaling at the box periphery.

The Ackland potential [19] is implemented to describe the interatomic forces present between Fe atoms, the details of which can be found in [18]. Although the Ackland potential has been found to overestimate the melting point, the potential produces reasonable estimates for values such as the bcc lattice parameter and the latent heat. Empirical potentials in general are limited due to their lack of including magnetism which plays a fundamental role in determining interatomic interactions such that even better potentials which have been recently developed [23] are limited. Even with its limitations, implementation of the Ackland potential is still a valid empirical potential method to study bcc Fe.

3. Results

The void is artificially produced as a result of a displacement cascade, shown in Fig. 1(a), which is situated at a GB region, in this case a TJ (blue arrow), in the unrelaxed sample. The movement of atoms is indicated by white lines which are superimposed on top of part of the sample, where atoms are represented by blue spheres. The SIAs produced as a consequence of this displacement cascade are attracted to the large regions of free volume between grains, some of which are pointed out by red arrows. Such a cascade differs from cascades in a relaxed sample because of the large areas of free, unstructured volume between grains in the unrelaxed sample that can accommodate SIAs. Fig. 1(b) shows a displacement cascade which occurs in the unrelaxed sample. Here the atoms of the sample are pictured using their potential energy, where red represents atoms with a potential energy greater than -4.0 eV and purple represents atoms with a potential energy less than -4.15 eV. The displacement cascade of Fig. 1(a), is again shown in Fig. 1(b) (i–iii). The TJ region in its initial state (i), forms a large atom-less area within the first MD time step (ii), due to the exodus of SIAs to the GBs, which collapses into a void. This void structure becomes and remains stable very early on in the 150 ps relaxation period. The relaxed void and surrounds are pictured in (iii).

A section of the relaxed structure containing the void and another relaxed sample containing the same number of atoms, which is void free, are pictured in Fig. 2(a) and (b) respectively. The spheres

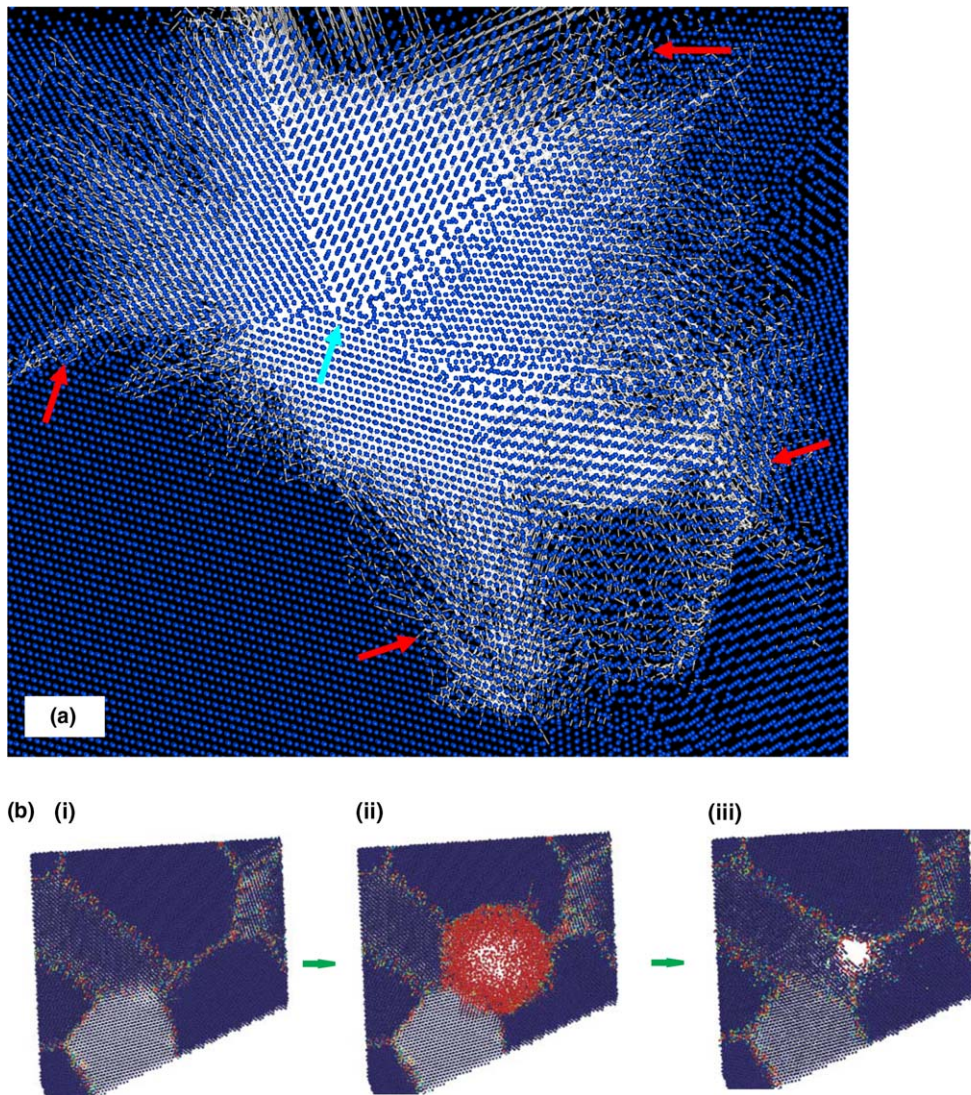


Fig. 1. (a) Ten nanometer section showing the movement of atoms during the displacement cascade, indicated by white lines, introduced in the unrelaxed sample. (b) The same section, 16 nm in width, of (i) initial sample (ii) after the first MD timestep, (iii) 150 ps later, when the sample is relaxed.

in this figure and Figs. 3 and 5 are coloured by their potential energy as described for Fig. 1(b). The grain interiors are represented by atoms with low potential energy and are distinguishable as purple atoms. The section shown attempts to display the maximum diameter of the void which is indicated by the internal spherical region absent of atoms. Comparison of the two samples shows that the GB structures (represented by the higher potential energy red/blue/green/yellow atoms) are similar in thickness and energy. The sample containing the artificially constructed void has high energy atoms (red) situated at the void surface.

As a consequence of the inclusion of the void and the accommodation of the atoms, the volume of the sample box containing the void is slightly larger than the other relaxed sample with a 0.06% increase in volume during relaxation. With the exclusion of the void (which is 2.9 nm in diameter) volume from the box volume, the density of atoms in the sample compared with the single crystal is 99.32% whereas the density of the voidless sample to single crystal sample is 99.34%. This indicates that the inclusion of the void has been accommodated in the sample by the growth of the sample during relaxation such that the density remains almost the same.

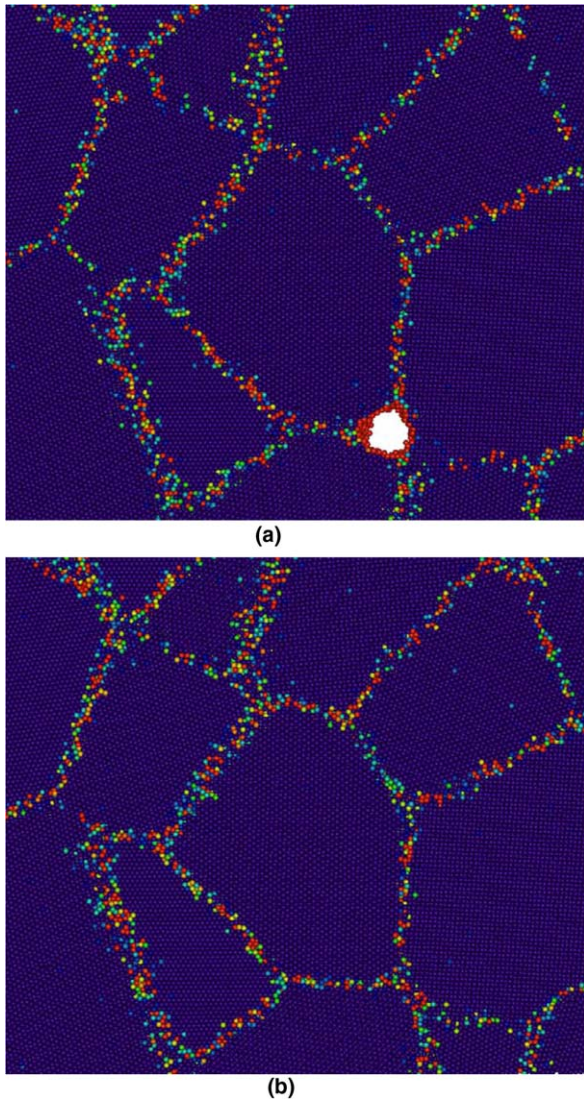


Fig. 2. Comparison of GB structures of nc bcc Fe sample, 26 nm in width and height (a) with a void structure (2.9 nm diameter) and (b) void free.

To obtain an estimate of how many vacancies such a void could contain, the initially created sample was compared with the relaxed void sample and the region of the void was found to contain 578 atoms. Such a void in a single crystal sample would be expected to contain 547 atoms. The excess number of atoms is expected to be due to the non-lattice GB atoms present.

Fig. 3 shows the relaxed sample with black lines superimposed to indicate the movement of atoms during a 20 keV PKA displacement cascade. From these atomic displacement lines, it can be seen that SIAs move both to the void and to GBs which are

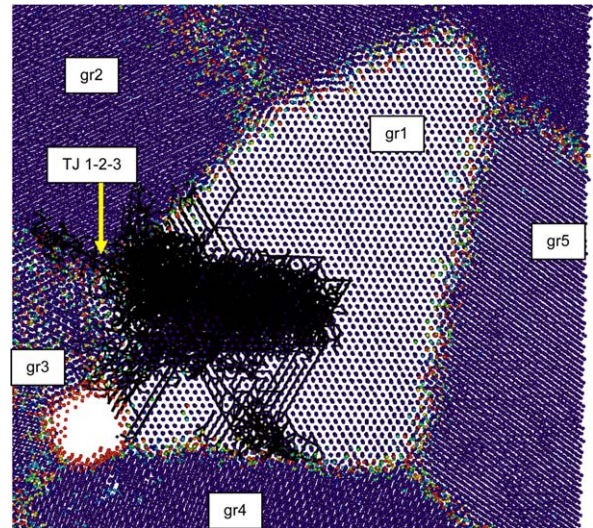


Fig. 3. Section of the relaxed sample with black lines showing the atomic displacement due to a 20 keV PKA. The grains (gr1-5) are labelled simply for reference, as is the triple junction (TJ) between grains 1–3. The width of GB1-4, excluding the void is 9.0 nm.

in close vicinity to the displacement cascade. As well as the main cascade, three subcascades form; one is located at the TJ1-2-3, another is in a neighbouring grain and one is situated near GB1-4. The void absorbs 23 SIAs which formed during the displacement cascade. The black lines indicate that the TJ, TJ1-2-3, has a large concentration of SIAs moving to it. This is due both to the proximity of the displacement cascade at the TJ and to the SIA sink attraction of the TJ; such attraction was also observed for nc fcc Ni TJs [24,25]. Comparison of the sink attraction of the void to that of the surrounding GBs, GB1-3 and GB1-4, indicates that the GBs have a similar sink attraction than the void. A section of GB1-4, adjacent to the void, is free of SIA movement making it clear that the SIAs in this region either go to the void or GB1-3 which is closer than GB1-4.

At the end of the displacement cascade the grains (two have been irradiated) contain 108 vacancies. One larger vacancy cluster has formed in the interior of one of the grains containing, according to the nearest neighbour criterion, 38 vacancies or containing 50 vacancies using a next to nearest neighbour criterion. This second description is included since 12 single vacancies sit in next to nearest neighbour positions at the periphery of the large vacancy structure forming what has been coined a ‘nascent vacancy cluster’ [26] which is expected to coalesce into one cluster over longer time [26]. Practically

all other vacancies present are single vacancies which, in the experimental timescale, will move quickly to the sink which attracts them the strongest. Experimentally, sinks in the form of dislocations have been observed to absorb SIAs while voids have absorbed vacancies leading to void growth [1]. The movement of the vacancy clusters produced in these simulations is outside of the scope of the MD time scale and the issue of void-vacancy and GB-vacancy interaction can not be addressed in this work.

Different aspects of SIA movement during the displacement cascade (black lines) are shown in Fig. 4(a) and (b), with grey spheres indicating atoms. In Fig. 4(a) the arrow is used to indicate atoms moving to the void so that it shrinks and the circle indicates where atoms move away from the void so that it grows. There is a larger movement of SIAs to the void coming directly from the displacement cascade (right arrow) but also from the rearrangement of a TJ area situated at the

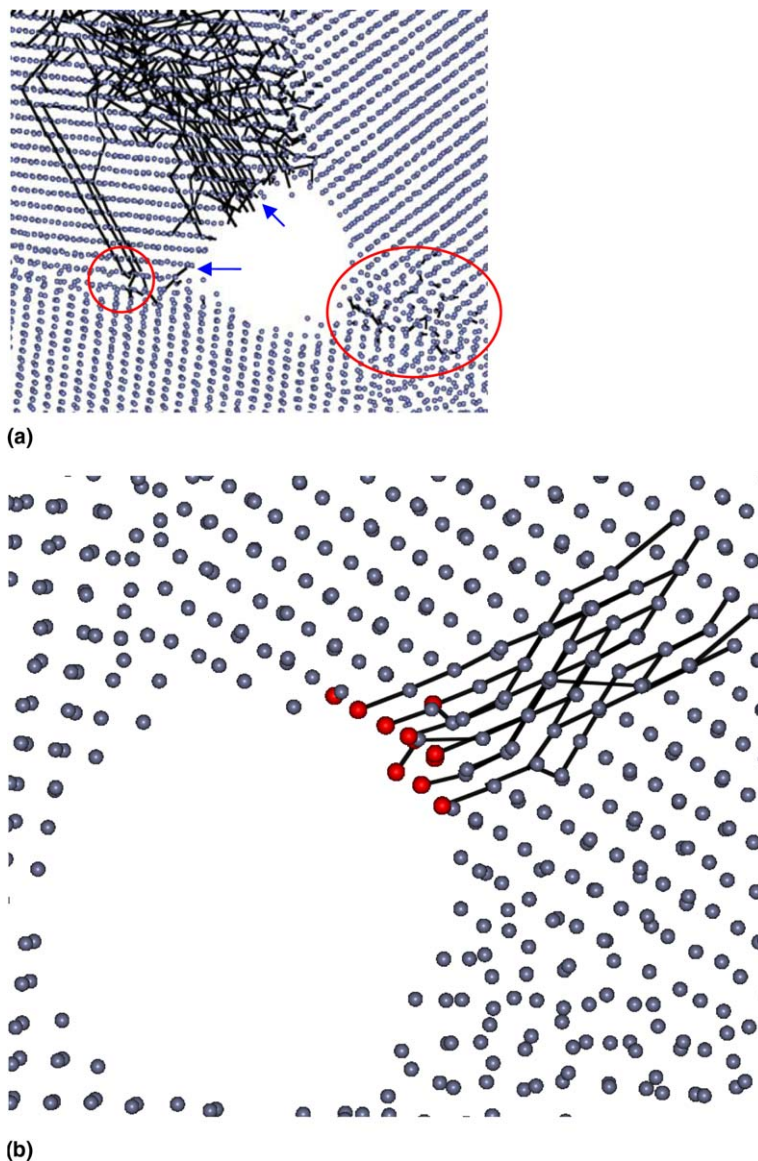


Fig. 4. A section of the sample where part of a 20 keV PKA cascade is shown with the displacement of atoms (black lines). The void is 2.9 nm in diameter. (a) Arrows indicate SIAs moving towards the void; circles indicate SIAs moving away from the void. (b) Red atoms indicate the additional atoms at the void periphery that align along the bcc structure of the grain and make the void shrink. (For interpretation of the color in this figure legend, the reader is referred to the web version of this article.)

periphery of the void. This shrinkage is, however, slowed by the movement of atoms away from the surface of the void (right circle) due to rearrangement within the neighbouring GB region. The left circle shows that some SIAs, even when they are in close proximity to the void prefer GB sinks present in the sample. It is interesting to see that the absorption of these SIAs at a GB leads to rearrangement of atoms within the GB region and to the consequent movement of GB atoms towards the void.

Of the SIAs that are produced 21% (23 of the 108 SIAs produced) move to the void structure. The other 85 SIAs move to GBs. Fig. 4(b) shows a section of the relaxed sample with black lines showing the movement of some of these SIAs to the void. The red spheres indicate SIAs which have moved to the void periphery by the end of the displacement cascade simulation. The SIAs move, change direction and then move to areas where the void is not completely spherical, filling it along the bcc lattice sites and making it slightly smaller. At the end of the displacement cascade the void is 2.8 nm in diameter in one direction and 2.9 nm in diameter in another direction. Discrepancies in measurement of the diameter occur because of the very local region where the void absorbs SIAs. Using the same estimation technique as above, a void 2.8 nm in diameter would be expected to contain 522 atoms. For a perfectly spherical void the addition of 23 bcc Fe atoms would decrease the diameter of the void from 2.9 to 2.86 nm which is difficult to estimate in these measurements of the diameter.

The introduction of a 5 keV PKA displacement cascade close to the void structure, again reveals that the strength of the void as a sink is small, with the absorption of merely three single SIAs. Other SIAs prefer to move 4.7 and 4.6 nm to GBs on the opposite side of the grain. This highly glissile nature is typical of bcc Fe SIAs, which leads to little clustering [27] and to their quick movement and absorption by surrounding sinks [18]. This displacement cascade has produced 57 Frenkel pairs. Of the 57 vacancies, 32 are single vacancies which will, in a time frame longer than this MD simulation, move to sinks. Of the 57 SIAs, 54 have moved to other GBs indicating that during this displacement cascade, the void has not acted as a strong sink for SIAs.

In Fig. 5, a 10 keV PKA displacement cascade is placed far from the void. The black lines, indicating the displacement cascade, show that the closest void to cascade core distance is 9.9 nm. At this distance there is no apparent attraction of SIAs to the void

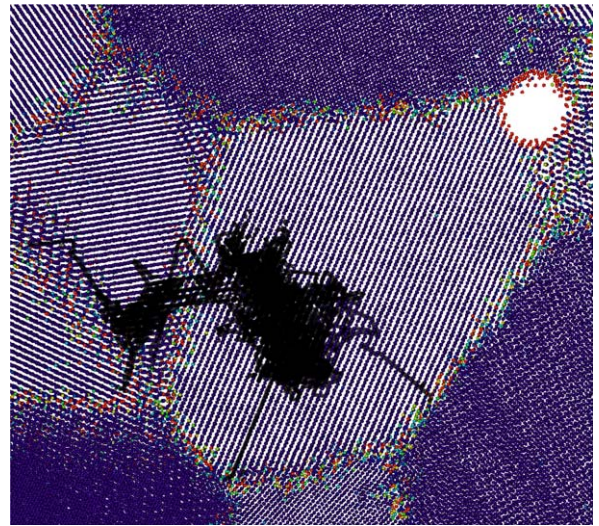


Fig. 5. A section of the relaxed sample with atomic displacement (black) due to a 10 keV PKA. The grain is 12.4 nm along the void to opposite side axis.

structure showing that the closer GBs are preferential SIA sinks. To obtain a more in-depth understanding of the void versus GB sink strength more displacement cascades with a variation of distance to the void will be performed.

4. Discussion and conclusion

The results presented here indicate that there are several different self interstitial atom mechanisms at play which influence the size of the void. Whether or not the strength of the sink attraction of the void is an artefact of the construction of the void itself and accuracy of the potential to describe these phenomena are factors which need to be kept in mind when considering these results.

During the displacement cascade, the nc structure forms larger numbers of single vacancies and larger vacancy clusters than its single crystal counterpart [18], indicating that a larger number of vacancies are present within the nc sample. The pre-existing void has absorbed self interstitial atoms, but has not completely annihilated with incoming SIAs. Its survival, along with the movement of at least 79% of other SIAs to GBs indicates that it may be a possible sink for vacancies left within the grains. Within the MD timescale, the void growth/shrinkage can only occur by the self interstitial atom movements, but what the vacancies would do if allowed the time to diffuse is still missing from the picture. Since small vacancy clusters

are highly mobile, their movement is very important in determining the shrinkage/growth of the void. In the fcc structure, large vacancy clusters form truncated stacking fault tetrahedra [28] in the presence of GBs. Such truncated stacking fault tetrahedra are stable structures, allowing MD simulations to provide a reasonable approximation of the displacement cascade. In the nc bcc structure, at the end of the MD simulation, there are a large number of vacancies left. Although stationary on the timescale of the MD simulation, these vacancies are highly mobile. The rearrangement that these vacancies will produce in a longer timeframe will indicate how the void size will progress.

Simulation of a pre-existing void in nc bcc Fe indicates that the void plays a role as a sink to self interstitial atoms during displacement cascades. Study of the self interstitial atoms shows that they also have an attraction for nearby GBs present in the sample. The role of vacancies, which is outside the MD timeframe, is seen to have an important role on the void and shows one of the limitation of MD simulations in studying voids. The origin of why and how the void attracts a certain number of self interstitial atoms, be it via its geometrical proximity to the simulated cascades or via its strain signature within the grain boundary network, will be a matter of further research.

Acknowledgements

Some of the present results were obtained as part of the EFDA Modelling of Fusion Materials Sub-task TW4-TTMS 007.

References

- [1] E. Kuramoto, T. Tsutsumi, *J. Nucl. Mater.* 212–215 (1994) 175.
- [2] M. Eldrup, B.N. Singh, *Mater. Sci. Forum* 363–365 (2001) 79.
- [3] M. Eldrup, B.N. Singh, *J. Nucl. Mater.* 276 (2000) 269.
- [4] C.A. English, *J. Nucl. Mater.* 108&109 (1982) 104.
- [5] B.N. Singh, M. Eldrup, S.J. Zinkle, S.I. Golubov, *Philos. Mag. A* 82 (2002) 1137.
- [6] J.A. Hudson, D.J. Mazey, R.S. Nelson, *J. Nucl. Mater.* 41 (1971) 241.
- [7] S.J. Zinkle, K. Farrell, *J. Nucl. Mater.* 168 (1989) 262.
- [8] M. Victoria, W.V. Green, B.N. Singh, T. Leffers, *J. Nucl. Mater.* 122&123 (1984) 737.
- [9] B.N. Singh, A. Horsewell, *J. Nucl. Mater.* 212–215 (1994) 410.
- [10] C.H. Woo, B.N. Singh, *Philos. Mag. A* 65 (1992) 889.
- [11] B.N. Singh, A.J.E. Foreman, *Philos. Mag. A* 66 (1992) 975.
- [12] H. Trinkaus, B.N. Singh, A.J.E. Foreman, *J. Nucl. Mater.* 206 (1993) 200.
- [13] N. Soneida, T. Diaz de la Rubia, *Philos. Mag. A* 78 (1998) 995.
- [14] S.L. Dudarev, *Phys. Rev. B* 65 (2002) 224105/1.
- [15] M. Samaras, P.M. Derlet, H. Van Swygenhoven, M. Victoria, *J. Nucl. Mater.* 323 (2003) 213.
- [16] M. Samaras, P.M. Derlet, H. Van Swygenhoven, M. Victoria, *Phys. Rev. B* 68 (2003) 224111/1.
- [17] S.L. Dudarev, A.A. Semenov, C.H. Woo, *Phys. Rev. B* 67 (2003) 0941031.
- [18] M. Samaras, P.M. Derlet, H. Van Swygenhoven, M. Victoria, *J. Nucl. Mater.*, in press, doi:10.1016/j.jnucmat.2006.02.030.
- [19] G.J. Ackland, D.J. Bacon, A.F. Calder, T. Harry, *Philos. Mag. A* 75 (1997) 713.
- [20] G.Z. Voronoi, *J. Reine, Angew. Math.* 1 (34) (1908) 199.
- [21] H. Van Swygenhoven, *Science* 296 (2002) 66.
- [22] H. Van Swygenhoven, D. Farkas, A. Caro, *Phys. Rev. B* 62 (2000) 831.
- [23] M.I. Mendeleev, S. Han, D.J. Srolovitz, G.J. Ackland, D.Y. Sun, M. Asta, *Philos. Mag. A* 83 (2003) 3977.
- [24] M. Samaras, P.M. Derlet, H. Van Swygenhoven, M. Victoria, *Philos. Mag.* 83 (2003) 3599.
- [25] M. Samaras, P.M. Derlet, H. Van Swygenhoven, M. Victoria, *Phys. Rev. Lett.* 88 (2002) 125505/1.
- [26] R.E. Stoller, *J. Nucl. Mater.* 276 (2000) 22.
- [27] Yu.N. Osetsky, A. Serra, B.N. Singh, S.I. Golubov, *Philos. Mag. A* 80 (2000) 2131.
- [28] M. Samaras, P.M. Derlet, H. Van Swygenhoven, M. Victoria, *Nucl. Instrum. and Meth. B* 202 (2003) 51.